PNAS RESEARCH ARTICLE | CELL BIOLOGY OPEN ACCESS

The UVSSA protein is part of a genome integrity homeostasis network with links to transcription-coupled DNA repair and ATM signaling

Magdalena M. Kordon[a,b,1], Sarah Arron[c], James E. Cleaver[c,2], Vladimir Bezrookove[d], Deneb Karentz[e], Brian Lu[c], Eli Perr[c], Darwin Chang[c], and Thoru Pederson[a]

Contributed by James E. Cleaver; received September 3, 2021; accepted February 2, 2022; reviewed by Karlene Cimprich and Yu-Ying He

The UVSSA (KIAA1530) protein is a component of transcription-coupled repair which, together with the CSA(ERCC8) and CSB(ERCC6) proteins cooperates to relieve transcription-blocking DNA damage. Mutations in *CSA* and *CSB* are found in Cockayne syndrome (CS), which is a human recessively inherited photosensitive, neurocutaneous, aging disorder. Mutations in *UVSSA*, in contrast, are found in the rare mild photosensitive syndrome (UV^s) that lacks the noncutaneous complications of CSA or CSB patients. In this study we deployed CRISPR to disrupt exon I of the *UVSSA* gene in the human embryonic kidney cell line HEK293. Elimination of the UVSSA protein was confirmed by Western blotting and the knockout cells displayed the predicted sensitivity to transcription blocking lesions caused by illudin, cisplatin, and ultraviolet light, just as in CS cell lines. Transcription arrest in a *UVSSA* knockout cell line resulted in ATM-dependent phosphorylation of H2Ax and delayed DNA synthesis, relieved by an inhibitor of ATM. Loss of UVSSA protein did not, however, increase sensitivity to oxidative damage or to inhibitors of poly (ADP)ribose polymerase, unlike reported in CSB cells. We discuss this in terms of the likely commutative interplay of factors in CS. We anticipate that this knockout cell line will advance understanding of this and possibly related transcription-coupled DNA repair diseases.

DNA repair | ATM | UVSSA | photosensitive syndrome | CRISP targeted deletion

Significance

Transcription-coupled repair (TCR) involves four core proteins: CSA, CSB, USP7, and UVSSA. CSA and CSB are mutated in the severe human neurocutaneous disease Cockayne syndrome. In contrast UVSSA is a mild photosensitive disease in which a mutated protein sequence prevents recruitment of USP7 protease to deubiquitinate and stabilize CSB. We deleted the UVSSA protein using CRISPR-Cas9 in an aneuploid cell line, HEK293, and determined the functional consequences. The knockout cell line was sensitive to transcription-blocking lesions but not sensitive to oxidative agents or PARP inhibitors, unlike CSB. Knockout of UVSSA also activated ATM, like CSB, in transcription-arrested cells. The phenotype of UVSSA, especially its rarity, suggests that many TCR-deficient patients and tumors fail to be recognized clinically.

Cockayne syndrome (CS) is a human recessively inherited neurocutaneous disorder that is defective in the transcription-coupled DNA repair (TCR) branch of nucleotide excision repair (NER). In addition, a mild disorder, ultraviolet (UV) sensitive syndrome (UV^s), and a severe neonatal lethal disorder, cranial ocular facial syndrome, represent extremes of mild and severe disorders also lacking TCR (1). Most cases exhibit mild to severe clinical photosensitivity but have never been reported to develop skin cancer (2, 3). CS therefore contrasts with xeroderma pigmentosum (XP), which lacks the global genome repair branch of NER but exhibits greatly elevated rates of skin cancer, both squamous cell carcinomas and melanomas (4). The different cancer phenotypes of these two branches of NER correlate with recent in vitro examination of fibroblasts: XP cells show increased rates of UV-induced mutagenesis whereas CS cells do not (5).

The hallmark of the CS family of disorders is seen in a reduced rate of recovery of RNA and DNA synthesis and apoptosis in patient-derived cells (6–8). The delayed recovery of RNA synthesis is due to prolonged arrest of RNA polymerase II at damaged bases and its release from the arrested transcription sites (9). The reduced recovery of DNA synthesis has several potential sources. Direct collision between R loops and replication forks may be one mechanism but would be confined to sites of simultaneous R loop formation and DNA replication forks (10). Indirect genome-wide inhibition of DNA synthesis has been proposed to be the result of activation of ATM kinase at sites of transcription arrest (11).

TCR involves at least four core proteins: CSA (ERCC8), CSB (ERCC6), UVSSA (KIAA1530), and USP7. TCR activates a cycle of ubiquitinylation and deubiquitinylation of CSB by the CSA ligase complex followed by recruitment of the USP7 protease by UVSSA (12). Although there has been extensive analysis of the phenotypes of mutations in *CSA* and *CSB* in response to transcription-blocking lesions and oxidative damage, less is known about the phenotype of mutations in *UVSSA*. This is because of the rarity of available fibroblast cell lines and the difficulty of recognizing the subtle clinical phenotype. An additional complication is that some mutations in XP and CS genes also give rise to the UV^s clinical phenotype (13, 14). For these reasons we sought to develop a cell line in which the *UVSSA* gene was inactivated by CRISPR-Cas9 targeting of the first coding exon. Here we report the success of this approach and describe

Author contributions: M.M.K., S.A., J.E.C., and T.P. designed research; M.M.K., J.E.C., V.B., D.K., B.L., E.P., and D.C. performed research; M.M.K. contributed new reagents/analytic tools; S.A., J.E.C., V.B., D.K., B.L., E.P., and T.P. analyzed data; and S.A., J.E.C., V.B., D.K., E.P., and T.P. wrote the paper.

Reviewers: K.C., Stanford University; and Y.-Y.H., University of Chicago.

The authors declare no competing interest.

[1]Present address: IntoDNA S.A., 30-38 Kraków, Poland.

[2]To whom correspondence may be addressed. Email: james.cleaver310@gmail.com.

This article contains supporting information online at http://www.pnas.org/lookup/suppl/doi:10.1073/pnas.2116254119/-/DCSupplemental.

Published March 7, 2022.

the resulting phenotype with respect to responses to a variety of DNA-damaging agents. We also deploy this knockout cell line to address roles of poly (ADP ribose) polymerase (PARP) and ATM. Our objectives were to determine 1) whether targeted knockout of the *UVSSA* gene in an aneuploid transformed cell line recapitulates the reported phenotype of UV^s, 2) to determine whether targeted knockout of *UVSSA* genes sensitizes cells to chemotherapy agents and 3) to inhibitors of PARP (PARPi), and 4) to determine whether the observed post-UV delay in DNA synthesis in the TCR-deficient UVSSA knockout cell is ATM-dependent.

Results

Three guide RNA constructs (named UVSSA-1, UVSSA-2, and UVSSA-3) targeting the first coding exon (exon II) were cloned into the vector lentiCRISPRv2 (15) (*SI Appendix*, Fig. S1). The functional impact of *UVSSA* gene inactivation on TCR was assessed based on the sensitivity of the cells to illudin (16) and UV light (*SI Appendix*, Fig. S2). Each of the UVSSA-inactivated cell lines was more sensitive than the parental cells, consistent with a deficiency in TCR (Fig. 1*B* and *SI Appendix*, Fig. S2). The parental cells' resistance to IIludin paralleled that reported previously with skin fibroblasts (Fig. 1*B*). Illudin is a fungal product that forms purine adducts in DNA that block transcription and require TCR for successful repair. The iilludin-purine adducts are not, however, sites for global genome repair (GGR). Cells lacking TCR are sensitive to illudin (e.g., CSA, CSB, and UV^s) but cells lacking GGR are not

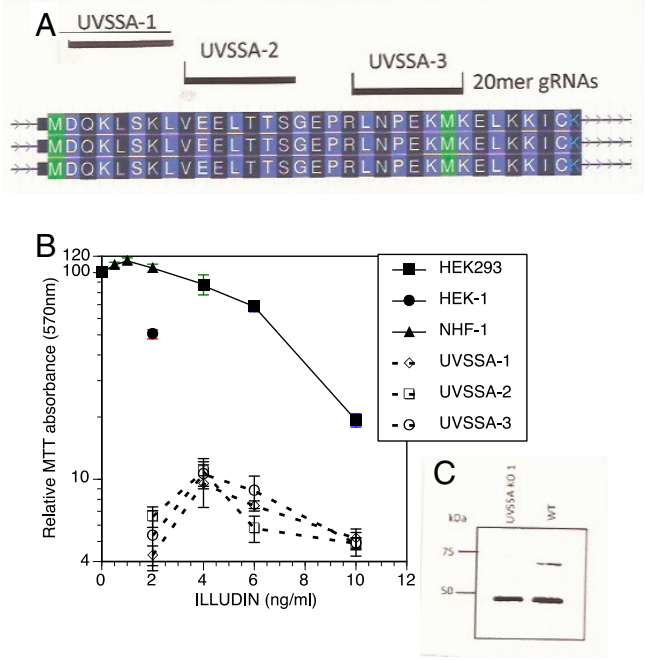

Fig. 1. Design of guide RNAs (gRNAs) and screen of targeted cell lines. (*A*) Amino acid sequence encoded by the first coding exon of *UVSSA* and locations of 3 gRNAs (UVSSA-1, UVSSA-2, and UVSSA-3). Green denotes the two putative translation start sites. (*B*) Relative survival of cloned cell lines to illudin. Solid squares: parental HEK293 (the low value at 2 ng/mL is ascribed to pipetting error but included for completeness; the data for HEK-1 cells was indistinguishable from HEK293). Open diamonds: UVSSA-1; open squares: UVSSA-2: open circles: UVSSA-3; closed triangles: NHF-1 human diploid fibroblasts. Means and SDs are shown (the SD for HEK293 is smaller than the symbol size), $n = 6$. (*C*) Western blot showing presence of UVSSA protein in HEK293 but its absence from UVSSA-1. Samples of equal protein concentration were loaded and β-actin was probed to serve as the loading control.

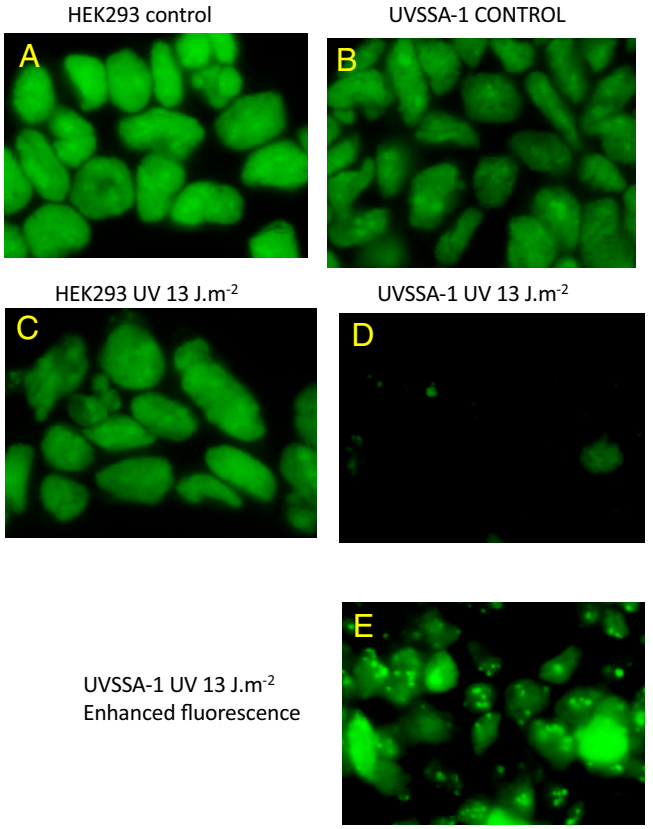

Fig. 2. RNA synthesis in HEK293 and UVSSA-1. Cells were labeled 24 h after UV (10 J·m^{-2}) for 1 h with 1 mM EU and stained with Alexa 488 fluor via a ClickIT reaction (see *Methods*). (*A*) HEK293 control. (*B*) HEK293 UV. (*C*) UVSSA-1 control. (*D*) UVSSA-1 UV. (*E*) UVSSA-1 UV with enhanced fluorescence to demonstrate apoptotic cells.

(e.g., XP-C and XP-E) (16). Little cell death was observed in HEK293 cells up to 6 ng/mL, with increased cell death at 10 ng/mL. In contrast, each of the UVSSA knockouts were killed at concentrations as low as 2 ng/mL. Since all three of the cell lines displayed similar UV hypersensitivity (*SI Appendix*, Fig. S2) only one of the lines, UVSSA-1, was used for the following studies. Further characterization of the knockout cells by Westerns or sequencing was not carried out, but emphasis was based on functional, phenotypic characterization.

RNA synthesis was determined 24 h after exposure to UV light by labeling cells with 5-ethynyluridine followed by fluorescence (Fig. 2 *A*–*E*). A dose of 13 J·m^{-2} had little impact on RNA synthesis in the parental cells but strongly suppressed RNA synthesis in UVSSA-1 cells (Fig. 2 *C*– *E*). Under increased microscopic illumination the UVSSA-1 cells showed an apoptotic morphology (Fig. 2*E*). This reduction in RNA synthesis is characteristic of TCR deficiency (17). These sensitivity assays together with the Western result (Fig. 1*C*) confirmed that we had inactivated the UVSSA alleles in this cell line.

UVSSA-1 cells had increased sensitivity to UVC light (Fig. 3*A* and *SI Appendix*, Fig. S2) and to cisplatin (Fig. 3*B*), consistent with the DNA damage induced by these agents being substrates for NER. UV photoproducts are substrates for both TCR and GGR (Table 1).

We have previously shown that the MTT viability assay produced anomalously high signals in TCR-deficient CSB cells exposed to the mitochondrial poison rotenone (18). This was interpreted to indicate that MTT and the CSB protein compete for electrons from complex I in the oxidative phosphorylation chain. Few significant anomalously high MTT signals were

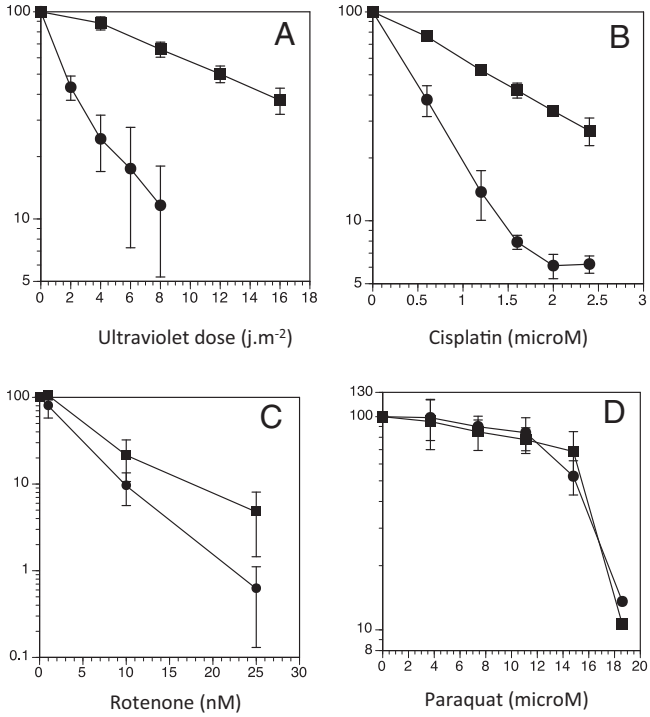

Fig. 3. Relative survival of HEK293 and UVSSA-1 after exposure to various toxic and DNA-damaging agents. (*A*) UV light (UVC). (*B*) Cisplatin. (*C*) Rotenone. (*D*) Paraquat. Means and SDs shown; $n = 6$ (*A*–*C*) or 12 (*D*). Solid squares: parental HEK293; solid circles: UVSSA-1.

observed in the UVSSA-1 cells (Fig. 3*C*), implying that UVSSA, unlike CSB, has no mitochondrial function. UVSSA-1 cells also showed no increased sensitivity to oxidative damage from paraquat (Fig. 3*D*), consistent with our previous results with hydrogen peroxide damage in hTERT fibroblasts in which UVSSA was down-regulated by short hairpin RNA (shRNA) (18).

We previously showed that CS cells, in addition to their phenotype of DNA damage-induced transcription arrest, were characterized by strong delays in DNA synthesis as well (6, 7) and no significant increase in UV mutagenesis above normal controls (5). We hypothesized that the delayed DNA replication was the cause of the lack of mutagenesis and that this delay could be caused by the noncanonical activation of ATM by CSB (11). The availability of our UVSSA-1 cell line gave us an opportunity to investigate this in a new way and examine the activation of ATM.

We investigated a target of ATM phosphorylation that is a marker of the DNA damage response together with use of an inhibitor of ATM (ATMi) in HEK293 and UVSSA-1 cells exposed to illudin (19, 20) As shown in Fig. 4 *C* and *D*, we observed that UVSSA-1 cells exposed to illudin activated ATM-dependent phosphorylation of γH2Ax, whereas much less activation was seen in HEK293 cells (Fig. 4 *A* and *B*). The immunofluorescence signals were subjected to statistical analysis by concentrating on single cells selected automatically as described in *Methods*. The asterisks denote the data used (see *SI Appendix*, Table S1).

We next tested whether the increased delay in DNA synthesis after UV light in UVSSA-1 cells was ATM-dependent. Cells that had been irradiated with 5.2 or 10.4 $J{\cdot}m^{-2}$ were grown for 24 h with or without ATMi and then labeled for 4 h with EdU (5-ethynyl-2′-deoxyuridine) and fixed. Cells were then processed with the ClickIT reaction to generate nuclear fluorescence levels that corresponded to levels of DNA synthesis. As with the previous experiments (Fig. 4 *A* and *B*), the immunofluorescence intensity was quantified using imageJ and plotted. Increasing doses of UV light depressed EdU labeling in both cell types but the effect of ATMi was different. Normal HEK293 cells did not respond to ATMi, indicating that ATM was not activated in these TCR-competent cells (Fig. 5), consistent with reports by Tresini et al. (11) in which TCR was inactive due to mutations in CSB. In UVSSA-1 cells, however, DNA synthesis was restored by ATMi, indicating that reduced DNA synthesis after UV irradiation was indirectly dependent on ATM signaling in UVSSA-1 cells (Fig. 5). As before, the signal intensities were subjected to statistical analysis with the asterisks denoting the data used (see *SI Appendix*, Tables S2 and S3).

CSB is a cofactor for base excision repair (BER) which results in sensitivity to oxidative DNA damage. UVSSA-1 cells were not, however, sensitive to paraquat (Fig. 3*D*), suggesting that UVSSA-1 does not participate in BER (21). PARP1 is an essential cofactor in BER and of repair of DNA breaks (22–24). Several early reports using first-generation inhibitors such as 3-aminobenzamide and 3,4-dihydro-5-[4-(piperidinyl)-butoxyl]-1(2H)-iso-quinolinone indicated that CSB cells were more sensitive than normal cells to inhibition of PARP. We used two more specific PARP inhibitors: talazoparib, which is NAD-like, and 5F02, which is unrelated to NAD (25). UVSSA-1 cells were not sensitive to either of these inhibitors of PARP (Fig. 6 *A* and *B*).

One possible explanation for these latter results could be the absence of PARP1 protein itself through possible off-target action of our original targeting. A major function of PARP1 is in the BER functions of CSB (24, 26–28), We therefore determined whether UVSSA cells retained PARP protein such that veliparib, another specific PARP inhibitor, would confer sensitivity when cells were exposed to the oxidizing agent paraquat. The observation that veliparib did sensitize UVSSA cells to paraquat (Fig. 6*C*) and cisplatin (Fig. 6*D*) demonstrated that these cells retained a functional PARP protein when exposed to exogenous DNA-damaging agents.

Table 1. Agents employed and modes of action

Agent	Major site of action	Mode
UV light	DNA photoproducts	GGR, TCR
Illudin	Guanine adducts	TCR
Cisplatin	DNA cross-links (inter, intra)	TCR
Paraquat	Oxidative damage	Single-strand DNA breaks, base excision
Rotenone	Complex I mitochondria	CSB electron sink
ATM kinase inhibitor KU60019	ATM	Double-strand breaks, oxidative damage
Veliparib (ABT888), 5F02,Talazoparib	PolyADP ribose polymerase	Single-strand DNA breaks, base excision

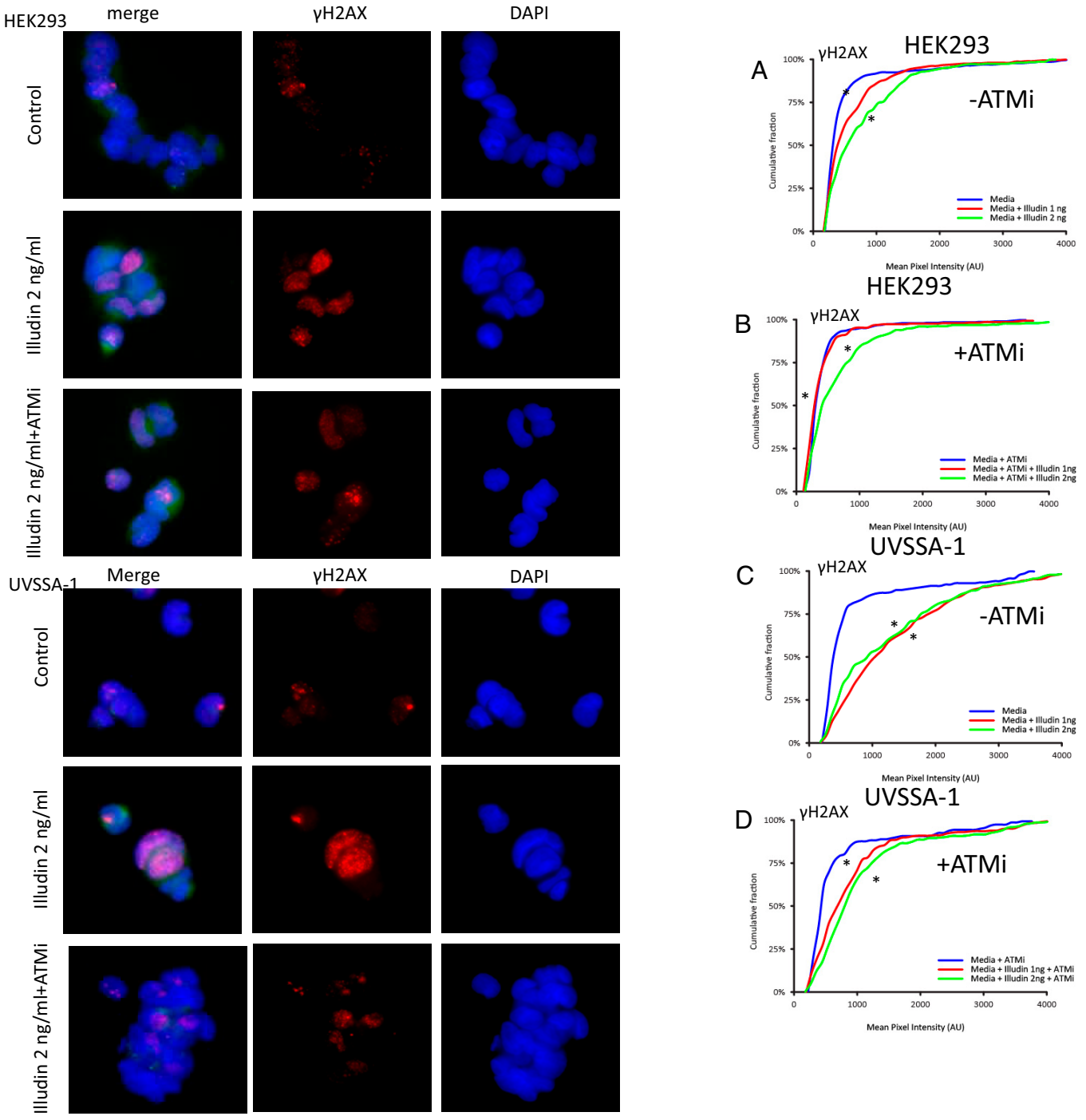

Fig. 4. Immunofluorescence in HEK293 and UVSSA-1 cells stained with antibody to γH2Ax fixed after exposure to illudin for 6 h. *Top*: HEK293 cells. Rows: control, illudin 2 ng/mL, illudin 2 ng/mL plus ATMi. Columns (left to right): merged images, γH2Ax, DAPI. *Bottom*: UVSSA-1 cells. Rows, control, illudin 2 ng/mL, illudin 2 ng/mL plus ATMi. Columns (left to right): merged images, γH2Ax, DAPI. (*A*–*D*) Immunofluorescence in HEK293 and UVSSA-1 cells fixed after exposure to illudin for 6 h and stained with γH2Ax antibody: (*A*) HEK293 cells exposed to illudin, (*B*) HEK293 cells exposed to illudin and ATMi for 6 h, (*C*) UVSSA-1 cells exposed to Illudin for 6 h, and (*D*) UVSSA-1 cells exposed to illudin and ATMi for 6 h. Asterisks denote comparisons for calculation of *P* values (see *SI Appendix*, Table S1).

Discussion

The UV-sensitive syndrome is a mild photosensitive disorder in which a terminal protein on the TCR pathway is mutated. Mutations in the *CSA* and *CSB* TCR genes are associated with symptoms of a range of severity of neurodevelopmental, segmental aging, and photosensitivity (1). In contrast, UV^s patients display only the photosensitive phenotype and no other symptoms have been reported (29, 30). The TCR deficiency is not significantly different in cells from CSA, CSB, or UV^s (1), but a striking feature of TCR deficiency is that these patients have never been reported to develop skin cancer despite having strong sunlight sensitivity (2, 3). In vitro, UV irradiation of TCR-deficient cells also does not cause mutations, as determined by duplex sequencing averaged over a range of genes of varied expression levels (5).

We chose to target the *UVSSA* gene because UV^s patients are rare and few fibroblast cell lines are available. We also

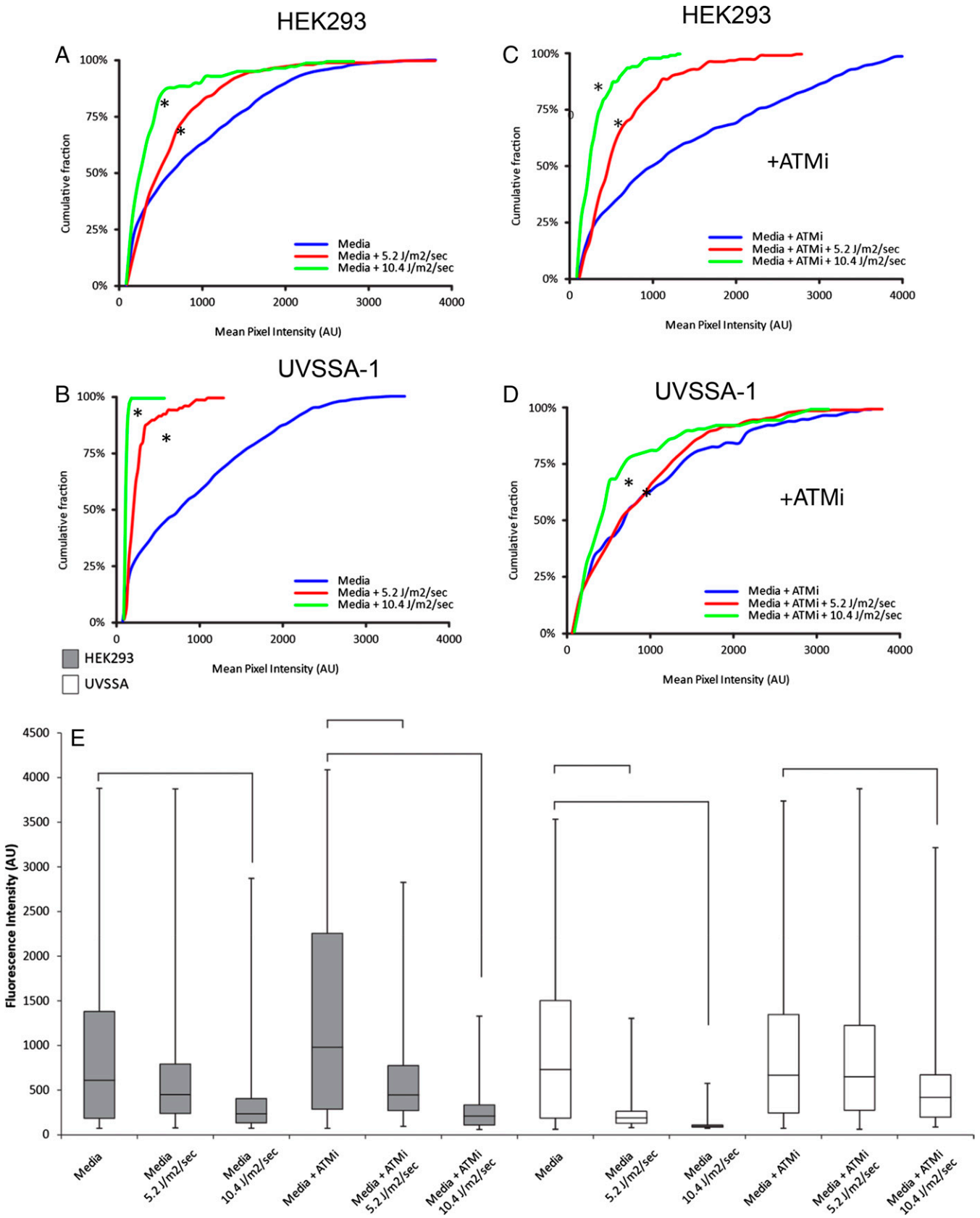

Fig. 5. Fluorescence in HEK293 and UVSSA-1 cells exposed to UV light grown for 20 h and then labeled with EdU for 4 h and stained with Alexa 488 fluor via a ClickIT reaction (see *Methods*). (*A* and *B*) Profiles for HEK293 cells irradiated with 5.2 and 10.4 J·m^{-2}·s^{-1} (4 and 8 s, respectively) (*A*) in medium alone or (*B*) in ATMi. (*C* and *D*) Profiles for UVSSA-1 cells irradiated with 5.2 and 10.4 J·m^{-2}·s^{-1} (4 and 8 s, respectively) (*C*) in medium alone or (*D*) grown in ATMi. (*E*) Box plots derived from the data in *A*–*D*. The box plots show the median and the first quartiles and the single vertical lines represent the maximum and minimum ranges. The *P* values were calculated for pairwise data indicated by asterisks (see *SI Appendix*, Table S2).

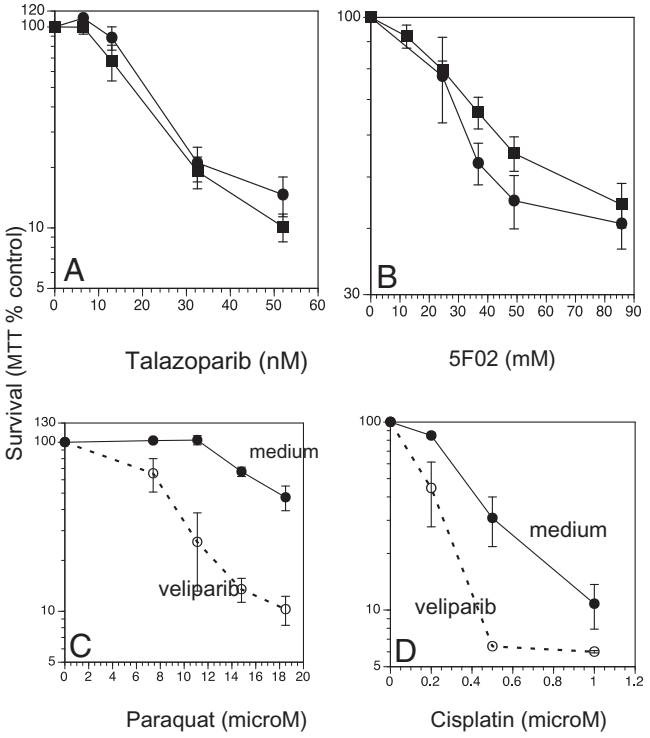

Fig. 6. Survival of HEK293 and UVSSA-1 cells exposed talazoparib (*A*) or SF02 (*B*). Solid squares: parental HEK293 cells; solid circles: UVSSA-1. Means and SDs are shown (n = 6 for *A*, n = 12 for *B*). Survival of HEK293 and UVSSA-1 cells exposed to (*C*) paraquat and grown in the presence or absence of veliparib (40 μm) or (*D*) to cisplatin and grown in the presence or absence of veliparib (40 μm). Solid squares: HEK293; open circles: paraquat UVSSA-1. Means and SDs are shown (n = 12).

wished to determine whether the use of CRISPR-Cas9 would be effective in aneuploid transformed cells. We previously examined the phenotype of hTERT transfected human fibroblasts in which *UVSSA* was inactivated by a shRNA (18). For the present study, we targeted the first coding exon of the *UVSSA* TCR gene for inactivation by CRISPR-Cas9. We successfully generated cell lines with the characteristic TCR-deficient phenotype of sensitivity to illudin and UV light and then carried out a detailed study with one of the lines, UVSSA-1. These cells displayed reduced RNA synthesis after DNA damage and were also sensitive to cisplatin, but not to rotenone or reactive oxygen species (ROS) from paraquat exposure. The latter is in contrast to CSA and CSB cells, which are sensitive to ROS, and where CSB acts as an electron sink for complex I of the mitochondria (18). Our results are also consistent with observations of efficient repair of oxidative damage in plasmids trafficked through UV^s but not CSB cells (21). The difference in the in vivo phenotypes of CSA and CSB as compared to UV^s patients therefore correlates with their increased sensitivity to oxidative damage rather than their common deficiency in TCR.

Transcription arrest has been shown to generate R-loops in which nascent RNA remains hybridized to the coding strand and the complementary strand remains single-stranded (31). The resulting structure might constitute a direct blockade to DNA synthesis and indirectly cause numerous downstream effects through noncanonical ATM activation, as previously demonstrated in CSB fibroblasts (11, 32). The block to DNA synthesis could be toxic and cause apoptosis, whereas ATM activation would have numerous downstream alterations in signal transduction and protein functions. We previously hypothesized that ATM could down-regulate DNA synthesis and thus prevent development of mutations by delayed replication of damaged sites (5, 33). We revealed the role of ATM in UVSSA knockout cells by demonstrating that persistent transcription arrest resulted in increased phosphorylation of γH2AX and its reduction by ATMi. We also observed that reduced DNA synthesis in the knockout cells after UV light was reversed by ATMi. This confirmed our earlier hypothesis that DNA synthesis was ATM-dependent in TCR-deficient cells. Since HEK293 cells are TCR-competent they do not experience a transcription arrest and so do not activate ATM (Fig. 5), which requires the arrest of transcription and R-loop formation (11, 32).

We observed that two PARP inhibitors did not sensitize wild-type cells or the knockout cells in the absence of exogenous damage. This was not due to an absence of PARP in UVSSA cells since veliparib sensitized them to paraquat, an oxidizing agent, and to cisplatin, a chemotherapeutic agent. Previous work showed that CS cells have low levels of NAD^+ due to persistent PARP synthesis from endogenous oxidative damage (34, 35). This result contrasts with our earlier observation that veliparib sensitized cells to an alkylating agent but increased survival after exposure to cisplatin (36), thus showing that the response to PARPi can be very cell-type-dependent.

Veliparib is an NAD-like inhibitor of PARP (25) which is therefore likely to be a competitive inhibitor with the cellular pool of NAD itself. CSB-deficient cells are more sensitive to PARPi due to depletion of the NAD pool during continual PARP-dependent repair of endogenous ROS damage (34, 37). Supplementation of the cellular NAD has been shown to ameliorate numerous pathological symptoms in CSB mice (35, 37). UVSSA protein plays no role in BER (21), so the intracellular pool of NAD is unlikely to be depleted in UVSSA knockout cells.

In summary, we have shown that deletion of the UVSSA TCR protein elicits a set of TCR-dependent phenotypes similar to those seen in CSB-deficient cells, including inhibition of RNA synthesis and sensitivity to illudin, UV light, and cisplatin. The major differences in the pathology of human UV^S patients and CSB patients therefore does not lie in any difference in TCR but in other properties of the two proteins. Our current data and other published results (22, 37) indicate that these properties may involve chromatin remodeling (22) and PARP-dependent changes in the NAD pool (22, 24) due to deficient repair of oxidative damage (18, 21). In particular, low NAD levels may precipitate the aging and development pathology of CS patients. In contrast, maintaining high levels of NAD would be expected to prevent such pathology in those UV^S patients who appear to have only mild photosensitivity.

Methods

Cell Culture. Cell lines deficient in the transcription coupled repair gene *UVSSA* were generated using the CRISPR-Cas9 in the human embryo kidney cell line designated HEK293 or HEK-1 according to the source. The HEK-1 line was only used in initial screening (Fig. 1). According to the source (American Type Culture Collection) this cell line was transformed with the left arm of adenovirus type 5 DNA and is hypotriploid with modal chromosome number 64. Prominent chromosome rearrangements include der(1)*t* (1;15) (q42;q13), der(19)*t* (3;19) (q12;q13), and der(12)*t* (8;12) (q22;p13) and three copies of X chromosomes (paired of Xq+, and a single Xp+ in most cells). This cell line was chosen in order to focus on the roles of TCR deficiencies on replication and transcription delays characteristic of CS and UV^S genotypes.

Work with human cells was approved by the University of California, San Francisco Committee on Human Research (IRB11-05993).

CRISPR Knockouts. UVSSA knockout cell lines were created using CRISPR-Cas9. Guide RNAs were designed to target three different regions of the first coding exon of UVSSA (Fig. 1*A* and *SI Appendix*, Fig. S1) The targeted sequences were UVSSA-1 (GGATCAGAAACTTTCGAAGT), UVSSA-2 (GTAGAAGAGCTCACAACTTC), and UVSSA-3 (ACTAAATCCTGAGAAAATGA) (Fig. 1*A*). Following transient transfection and two rounds of selection in puromycin pairs of clones from the same transfection representing the same targeting site in the gene were isolated and clonally selected in puromycin as detailed in Fig. 1 and *SI Appendix*, Fig. S1. Illudin sensitivity measurements on the resulting cell lines showed that deletion of each targeted region had the same impact; most work was carried out using the cell line in which the most 5′-ward region of the exon was targeted (designated UVSSA-1).

For experiments on illudin sensitivity an additional primary human fibroblast cell line designated NHF-1 (gift of Dennis Oh, University of California, San Francisco, CA) was used for comparison.

Sensitivity to DNA-Damaging Agents. To measure UV survival, cells were grown for 24 h in 96-well plates, briefly drained of medium, and then exposed to a range of doses of UVC (254 nm, 1.3 J·m^{-2}). For sensitivity assays using cisplatin, oxidizing agents and inhibitors after chemical exposure 10-μL aliquots of each chemical at the desired stock concentrations were placed into wells of 96-well plates, after which cell suspensions (100 μL) were added. Cisplatin makes intrastrand cross-links between adjacent purines and despite some similarity to UV photoproducts these are mainly transcription-blocking adducts and not recognized in XP-C cells and so not repaired by GGR (38). The cells were then cultured for 5 to 7 d, by which time control wells were confluent and plates were assayed colorimetrically with 3-(4,5-dimethylthiazol-2-yl)-2,5-diphenyltetrazolium bromide (MTT; Sigma-Aldrich) at 570 nm (18). Relative survival was calculated from the ratios of exposed to unexposed wells, based on the average 570-nm absorbance in 6 or 12 wells per exposure condition; a single 96-well plate using either one cell type for the whole 96-well plate or two cell types per tray and three rows per cell type was used for each agent and dose range. The surviving cell numbers represent a combination of cell death, growth delays, and rates of regrowth. By ensuring that only the control wells reached confluence at the time of assay, relative absorbance was a measure of cell sensitivity that could be compared across agents and cell types. We find that the results obtained with the MTT assay became increasingly variable and unreliable at low levels of survival, so initial screens were confined to no more than the second log of sensitivity. Means and SDs are shown for $n = 6$ or $n = 12$.

Western Blots. For preparation of whole-cell protein lysates cells were washed with cold phosphate-buffered saline and lysed with cold RIPA buffer (Thermo Scientific, 89900) supplemented with protease and phosphatase inhibitors (Thermo Scientific, 78442) for 30 min at 4 °C. Lysates were clarified by centrifugation at 12,000 rpm for 20 min at 4 °C to pellet cell debris. The supernatant was aspirated into a fresh tube on ice and the protein concentration measured.

For Western blotting equal amounts of protein were loaded prior onto sodium dodecyl sulfate polyacrylamide gel electrophoresis, followed by electrophoretic protein transfer to a poly(vinylidene difluoride) membrane. Protein transfer efficiency was confirmed using Ponceau S staining (Fisher Scientific, BP10310). The membrane was blocked with 5% blotting-grade nonfat milk in TBST (BioRad, 1706404) for 1 h at room temperature prior to probing with primary antibodies overnight at 4 °C and secondary antibodies for 1 h at room temperature. The membrane was incubated in Luminata Classico Western HRP substrate according to the manufacturer's instructions (EMD Millipore, WBLUC0500) then exposed to X-ray film and processed.

The antibodies used included primary β-actin antibody (C4, SC-47778) and secondary IgGκ BP-HRP antibody (SC-516102) from Santa Cruz Biotechnology. Primary UVSSA antibody (N1N2, GTX106751) and secondary rabbit IgG horseradish peroxidase (HRP)-conjugated antibody (GTX213110-01) were obtained from Genetex.

DNA and RNA Synthesis. DNA and RNA synthesis were assayed using the Click-IT reaction (Invitrogen). Cells were treated with various agents and labeled with either EdU for DNA synthesis or EU (5-ethynyl-uridine) for RNA synthesis. After labeling durations of up to 24 h cells were fixed in 3.7% formaldehyde and incubated with Alexa 488-conjugated antibodies for the incorporated modified nucleoside covalently linked to the corresponding group in DNA or RNA according to the manufacturer's instructions. The stained slides were examined and subjected to quantitative fluorescence microscopy.

Protein Immunofluorescence. Cells were fixed at 4 h and stained with an antibody against γH2Ax as described in the figure legends. Expression of the protein was assessed using immunofluorescence performed on cells cultured on coverslips as previously described (36). Antibody against γH2AX (at 1:1,000 dilution; EMD Millipore) were detected using secondary antibodies labeled with Alexa Fluor 488 and 594 (1:1,000 dilution; Lifetech). DAPI staining was used to counterstain the nuclei. Due to the tendency of the cells to clump they were scored automatically rather than manually. A region of interest around a fixed image of a single cell stained with DAPI was defined for automatic cell scoring, with images larger or smaller discarded. Images were taken at fixed exposures with a Zeiss Axio Image Z2 microscope and the fluorescence intensities of individual cells were quantified using ImageJ software. The mean pixel intensities were used for subsequent statistical analysis using Microsoft Excel and Data Desk. The statistical analyses performed with either two-sample Kolmogorov–Smirnov or Mann–Whitney *U* tests, as indicated in *SI Appendix*, Tables S1–S3.

Data Availability. All study data are included in the article and/or *SI Appendix*. Cell lines used will be available on request.

ACKNOWLEDGMENTS. This work was supported by the University California, San Francisco Mount Zion Health Fund award ID 018132/P0531999 (S.A.), the E. A. Dickinson Emeritus Professorship of University California, San Francisco (J.E.C.) Project Number 7501288, and the Lily Drake Cancer Research Fund, account 252175 from the University of San Francisco (J.E.C. and D.K.). M.M.K. was a recipient of a doctoral studentship awarded by the Polish National Science Center (2015/16/T/NZ3/00157). T.P. was supported by NIH U01 DA 040588 (Paul Kaufman and Job Dekker, Co-Principal Investigators). We thank Dr. M. Kashani-Sabet (California Pacific Medical Center, San Francisco) for use of his facilities for quantitative fluorescence microscopy and his support and advice and Drs. David Semir and Altaf Dar for numerous technical suggestions. We thank Dr. Hanhui Ma in the T.P. laboratory for strategy on the CRISPR inactivation. Dr. Cynthia Myers (Fox Chase Cancer Center) kindly donated a sample of the PARP inhibitor SF02.

Author affilitions: [a]Department of Biochemistry and Molecular Biotechnology, University of Massachusetts Chan Medical School, Worcester, MA 01605; [b]Department of Cell Biophysics, Faculty of Biochemistry, Biophysics, and Biotechnology, Jagiellonian University, 30-387 Kraków, Poland; [c]Department of Dermatology, University of California, San Francisco, CA 94122; [d]California Pacific Medical Center Research Institute, San Francisco, CA 94107; and [e]Department of Biology, University of San Francisco, San Francisco, CA 94117

1. V. Laugel, Cockayne syndrome: The expanding clinical and mutational spectrum. *Mech. Ageing Dev.* **134**, 161–170 (2013).
2. W. R. Zhang, G. L. Garrett, S. T. Arron, J. E. Cleaver, Survey of Cockayne patients reports no skin cancers despite DNA repair deficiency. *J. Am. Acad. Dermatol.* **74**, 1270–1272 (2016).
3. M. A. Nance, S. A. Berry, Cockayne syndrome: Review of 140 cases. *Am. J. Med. Genet.* **42**, 68–84 (1992).
4. K. H. Kraemer, M. M. Lee, A. D. Andrews, W. C. Lambert, The role of sunlight and DNA repair in melanoma and nonmelanoma skin cancer. The xeroderma pigmentosum paradigm. *Arch. Dermatol.* **130**, 1018–1021 (1994).
5. K. S. Reid-Bayliss, S. T. Arron, L. A. Loeb, V. Bezrookove, J. E. Cleaver, Why Cockayne syndrome patients do not get cancer despite their DNA repair deficiency. *Proc. Natl. Acad. Sci. U.S.A.* **113**, 10151–10156 (2016).
6. A. R. Lehmann, S. Kirk-Bell, L. Mayne, Abnormal kinetics of DNA synthesis in ultraviolet light-irradiated cells from patients with Cockayne's syndrome. *Cancer Res.* **39**, 4237–4241 (1979).
7. J. E. Cleaver, Normal reconstruction of DNA supercoiling and chromatin structure in cockayne syndrome cells during repair of damage from ultraviolet light. *Am. J. Hum. Genet.* **34**, 566–575 (1982).
8. L. V. Mayne, A. R. Lehmann, Failure of RNA synthesis to recover after UV irradiation: An early defect in cells from individuals with Cockayne's syndrome and xeroderma pigmentosum. *Cancer Res.* **42**, 1473–1478 (1982).
9. Y. Y. Chiou, J. Hu, A. Sancar, C. P. Selby, RNA polymerase II is released from the DNA template during transcription-coupled repair in mammalian cells. *J. Biol. Chem.* **293**, 2476–2486 (2018).
10. M. P. Crossley, M. Bocek, K. A. Cimprich, R-loops as cellular regulators and genomic threats. *Mol. Cell* **73**, 398–411 (2019).
11. M. Tresini *et al.*, The core spliceosome as target and effector of non-canonical ATM signalling. *Nature* **523**, 53–58 (2015).
12. P. Shah, Y.-Y. He, Molecular regulation of UV-induced DNA repair. *Photochem. Photobiol.* **91**, 254–264 (2015).

13. P. K. Cooper, T. Nouspikel, S. G. Clarkson, S. A. Leadon, Defective transcription-coupled repair of oxidative base damage in Cockayne syndrome patients from XP group G. *Science* **275**, 990–993 (1997).
14. T. Nardo *et al.*, A UV-sensitive syndrome patient with a specific CSA mutation reveals separable roles for CSA in response to UV and oxidative DNA damage. *Proc. Natl. Acad. Sci. U.S.A.* **106**, 6209–6214 (2009).
15. N. E. Sanjana, O. Shalem, F. Zhang, Improved vectors and genome-wide libraries for CRISPR screening. *Nat. Methods* **11**, 783–784 (2014).
16. N. G. Jaspers *et al.*, Anti-tumour compounds illudin S and Irofulven induce DNA lesions ignored by global repair and exclusively processed by transcription- and replication-coupled repair pathways. *DNA Repair (Amst.)* **1**, 1027–1038 (2002).
17. A. R. Lehmann, Three complementation groups in Cockayne syndrome. *Mutat. Res.* **106**, 347–356 (1982).
18. J. E. Cleaver *et al.*, Mitochondrial reactive oxygen species are scavenged by Cockayne syndrome B protein in human fibroblasts without nuclear DNA damage. *Proc. Natl. Acad. Sci. U.S.A.* **111**, 13487–13492 (2014).
19. M. M. Kordon *et al.*, PML-like subnuclear bodies, containing XRCC1, juxtaposed to DNA replication-based single-strand breaks. *FASEB J.* **33**, 2301–2313 (2019).
20. K. N. Choe *et al.*, HUWE1 interacts with PCNA to alleviate replication stress. *EMBO Rep.* **17**, 874–886 (2016).
21. G. Spivak, P. C. Hanawalt, Host cell reactivation of plasmids containing oxidative DNA lesions is defective in Cockayne syndrome but normal in UV-sensitive syndrome fibroblasts. *DNA Repair (Amst.)* **5**, 13–22 (2006).
22. J. C. Newman, A. D. Bailey, A. M. Weiner, Cockayne syndrome group B protein (CSB) plays a general role in chromatin maintenance and remodeling. *Proc. Natl. Acad. Sci. U.S.A.* **103**, 9613–9618 (2006).
23. T. Stevnsner, M. Muftuoglu, M. D. Aamann, V. A. Bohr, The role of Cockayne Syndrome group B (CSB) protein in base excision repair and aging. *Mech. Ageing Dev.* **129**, 441–448 (2008).
24. T. Thorslund *et al.*, Cooperation of the Cockayne syndrome group B protein and poly(ADP-ribose) polymerase 1 in the response to oxidative stress. *Mol. Cell. Biol.* **25**, 7625–7636 (2005).
25. Y. Karpova *et al.*, Non-NAD-like PARP-1 inhibitors in prostate cancer treatment. *Biochem. Pharmacol.* **167**, 149–162 (2019).
26. A. Sakai, R. Sakasai, Y. Kakeji, H. Kitao, Y. Maehara, PARP and CSB modulate the processing of transcription-mediated DNA strand breaks. *Genes Genet. Syst.* **87**, 265–272 (2012).
27. C. Flohr, A. Bürkle, J. P. Radicella, B. Epe, Poly(ADP-ribosyl)ation accelerates DNA repair in a pathway dependent on Cockayne syndrome B protein. *Nucleic Acids Res.* **31**, 5332–5337 (2003).
28. H. Menoni *et al.*, The transcription-coupled DNA repair-initiating protein CSB promotes XRCC1 recruitment to oxidative DNA damage. *Nucleic Acids Res.* **46**, 7747–7756 (2018).
29. T. Itoh, Y. Fujiwara, T. Ono, M. Yamaizumi, UVs syndrome, a new general category of photosensitive disorder with defective DNA repair, is distinct from xeroderma pigmentosum variant and rodent complementation group I. *Am. J. Hum. Genet.* **56**, 1267–1276 (1995).
30. Y. Fujiwara, M. Ichihashi, Y. Kano, K. Goto, K. Shimizu, A new human photosensitive subject with a defect in the recovery of DNA synthesis after ultraviolet-light irradiation. *J. Invest. Dermatol.* **77**, 256–263 (1981).
31. J. Sollier, K. A. Cimprich, R-loops breaking bad. *Trends Cell Biol.* **25**, 514–522 (2015).
32. I. Klusmann *et al.*, Chromatin modifiers Mdm2 and RNF2 prevent RNA:DNA hybrids that impair DNA replication. *Proc. Natl. Acad. Sci. U.S.A.* **115**, E11311–E11320 (2018).
33. J. E. Cleaver, Transcription coupled repair deficiency protects against human mutagenesis and carcinogenesis: Personal Reflections on the 50th anniversary of the discovery of xeroderma pigmentosum. *DNA Repair (Amst.)* **58**, 21–28 (2017).
34. Y. Fujiwara, K. Goto, Y. Kano, Ultraviolet hypersensitivity of Cockayne's syndrome fibroblasts. Effects of nicotinamide adenine dinucleotide and poly(ADP-ribose) synthesis. *Exp. Cell Res.* **139**, 207–215 (1982).
35. M. Scheibye-Knudsen *et al.*, A high-fat diet and NAD(+) activate Sirt1 to rescue premature aging in cockayne syndrome. *Cell Metab.* **20**, 840–855 (2014).
36. I. Revet *et al.*, Functional relevance of the histone gammaH2Ax in the response to DNA damaging agents. *Proc. Natl. Acad. Sci. U.S.A.* **108**, 8663–8667 (2011).
37. J.-H. Lee *et al.*, Cockayne syndrome group B deficiency reduces H3K9me3 chromatin remodeler SETDB1 and exacerbates cellular aging. *Nucleic Acids Res.* **47**, 8548–8562 (2019).
38. T. Furuta *et al.*, Transcription-coupled nucleotide excision repair as a determinant of cisplatin sensitivity of human cells. *Cancer Res.* **62**, 4899–4902 (2002).